Published in final edited form as:

ACS Chem Biol. 2017 March 17; 12(3): 682–691. doi:10.1021/acschembio.6b01071.

Biosynthesis of the methylthioxylose capping motif of lipoarabinomannan in *Mycobacterium tuberculosis*

Shiva kumar Angala[‡], **Michael R. McNeil**[‡], **Libin Shi**[‡], **Maju Joe**[¶], **Ha Pham**[‡], **Sophie Zuberogoitia**[§], **Jérôme Nigou**[§], **Claudia M. Boot**[#], **Todd L. Lowary**[¶], **Martine Gilleron**[§], and **Mary Jackson**[‡]

[‡]Mycobacteria Research Laboratories, Department of Microbiology, Immunology and Pathology, Colorado State University, Fort Collins, CO 80523-1682, USA

[§]Institut de Pharmacologie et de Biologie Structurale, Université de Toulouse, CNRS, UPS, 205 route de Narbonne, F-31077 Toulouse, France

[#]Central Instrumentation Facility, Department of Chemistry, Colorado State University, Fort Collins, CO 80523-1872, USA

[¶]Alberta Glycomics Centre and Department of Chemistry, The University of Alberta, Edmonton, AB, T6G 2G2, Canada

Abstract

Lipoarabinomannan (LAM) is a lipoglycan found in abundant quantities in the cell envelope of all mycobacteria. The non-reducing arabinan termini of LAM display species-specific structural micro-heterogeneity that impacts the biological activity of the entire molecule. *Mycobacterium tuberculosis*, for instance, produces mannoside caps made of one to three α-(1→2)-Man*p*-linked residues that may be further substituted with an α-(1→4)-linked methylthio-D-xylose (MTX) residue. While the biological functions and catalytic steps leading to the formation of the mannoside caps of *M. tuberculosis* LAM have been well established, the biosynthetic origin and biological relevance of the MTX motif remain elusive. We here report on the discovery of a five-gene cluster dedicated to the biosynthesis of the MTX capping motif of *M. tuberculosis* LAM, and on the functional characterization of two glycosyltransferases, MtxS and MtxT, responsible, respectively, for the production of decaprenyl-phospho-MTX (DP-MTX) and the transfer of MTX from DP-MTX to the mannoside caps of LAM. Collectively, our NMR spectroscopic and mass spectrometric analyses of *mtxS* and *mtxT* overexpressors and knock-out mutants support a biosynthetic model wherein the conversion of 5′-methylthioadenosine, which is an ubiquitous byproduct of spermidine biosynthesis, into 5′-methylthioribose-1-phosphate precedes the formation of a 5′-methylthioribose nucleotide sugar, followed by the epimerization at C-3 of the

To whom correspondence should be addressed: Mary Jackson, Department of Microbiology, Immunology and Pathology, Colorado State University, Fort Collins, CO 80523-1682, Telephone (970) 491-3582; Fax: (970) 491-1815; Mary.Jackson@colostate.edu.

Author Contributions

S. k. A., M. Joe, M. G., M. J., M. R. M., J. N. and T. L. L. conceived the study. M. J., M. R. M., J. N. and T. L. L. coordinated the study. S. k. A., M. J., M. R. M., C. M. B. and M. G. wrote the paper. S. k. A., L. S. and H. P. constructed and analyzed recombinant mycobacterial strains. S. k. A., S. Z., C. M. B., M. R. M. and M. G. analyzed the cell envelope composition of the recombinant strains and performed the NMR experiments. All authors reviewed the results and approved the final version of the manuscript.

Supporting Information Available - This material is available free of charge *via* the Internet.

ribose residue, and the transfer of MTX from the nucleotide sugar to decaprenyl-phosphate yielding the substrate for transfer onto LAM. The conservation of the MTX biosynthetic genes in a number of Actinomycetes suggests that this discrete glycosyl substituent may be more widespread in prokaryotes than originally thought.

Keywords

Mycobacterium; tuberculosis; lipoarabinomannan; methylthioxylose

INTRODUCTION

The mycobacterial cell envelope is characterized by its high content of mannosylated molecules. The mannosyl-phosphatidyl-*myo*-inositol-based glycolipids (PIMs) and metabolically related lipoglycans comprising lipomannan (LM) and lipoarabinomannan (LAM), in particular, are found in abundant quantities in the inner and outer membranes of all mycobacterial species (1–2). The most common forms of LM and LAM share a linear α-(1→6)-linked mannan backbone made up on average of 20–25 mannopyranose (Man*p*) residues occasionally substituted at C-2 by single Man*p* units (3). The major LAM glycoforms contain about 110 glycosyl residues (approximately 60 Ara*f* and 50 Man*p* units) and consist of a single D-arabinan chain attached to the α-(1→6) D-mannan backbone (4). The arabinan polymer contains about 60 Ara*f* units and consists of a linear α-(1→5)-linked Ara*f* backbone punctuated with branched hexaarabinofuranosides (Ara_6) and linear tetraarabinofuranosides (Ara_4) (5). Succinate or lactate residues may substitute the C-2 position of some of the α-(3→5)-Ara*f* interior residues of the arabinan (6–7). Importantly, the non-reducing arabinan termini of LAM display considerable species-specific structural micro-heterogeneity that is key to the biological activity of the entire molecule (8–11). *M. tuberculosis* and other pathogenic slow-growing mycobacteria (*M. bovis, M. leprae, M. avium, M. xenopi, M. marinum* and *M. kansasii*), for instance, produce mannoside caps made of one to three α-(1→2)-Man*p*-linked residues giving rise to mannosylated LAM (referred to as ManLAM). Intriguingly, the mannoside caps of ManLAM of all *M. tuberculosis* isolates analyzed to date may be further substituted with an α-(1→4)-linked methylthio-D-xylose (MTX) residue [Fig. 1] (12–16). The same MTX motif apparently substitutes the ManLAM of *M. avium* and *M. kansasii* although, in the latter species, its attachment is to the mannan backbone rather than to the non-reducing termini of the arabinan domain (8,15,17). MTX is a discrete motif that occurs at the level of one molecule per entire molecule of ManLAM in *M. tuberculosis* (or one molecule for every five to six mannose caps) (12,18). It is unusual in that it is one of the few reports of a *xylo*-configured sugar outside the plant kingdom and the first report of a thiosugar in a bacterial polysaccharide (16). The biosynthetic origin of this motif is unknown although models have been proposed (12,14,16).

The conservation of the MTX motif of ManLAM in *M. tuberculosis* and other pathogenic mycobacteria and its exposure on the cell surface suggest that it may play a beneficial role to the bacterium in host-pathogen interactions. Accordingly, *in vitro* studies indicate that disaccharide mimetics of the MTX capping motif of ManLAM downregulate cytokine

production by activated human macrophages in culture (15) and that the MTX motif of purified ManLAM may account for the anti-oxidative properties of the lipoglycan (18–19). To what extent these properties impact the interactions of intact *M. tuberculosis* bacilli with phagocytic cells and the immunopathogenesis of tuberculosis (TB) remains to be determined.

With the goals of elucidating the biosynthetic pathway leading to the formation of the MTX motif of ManLAM and of generating isogenic MTX-deficient *M. tuberculosis* mutants that subsequently could be used to investigate the biological relevance of this motif in TB infection, a combination of genetic and (bio)chemical approaches was here used to identify the enzymes responsible for the synthesis and transfer of the MTX motif to the *t*-Man*p* residue of the mannoside caps of ManLAM.

RESULTS AND DISCUSSION

Identification of a gene cluster potentially involved in the biosynthesis of the MTX substituent of ManLAM in M. tuberculosis

It has been postulated that the MTX motif was likely to be derived biosynthetically from 5′-methylthioadenosine (MTA), which is a ubiquitous byproduct of spermidine biosynthesis (12,15–16). MTA is toxic to the cells and is therefore rapidly converted to adenine and 5′-methylthioribose-1-phosphate, which may be used in the purine and methionine salvage pathways, respectively. Whereas this conversion is catalyzed by an MTA phosphorylase (MTAP, E.C 2.4.2.28) in Eukarya, bacteria rely on the coupled action of an MTA nucleosidase (MTAN, E.C 3.2.2.16) and a kinase. *Mycobacterium smegmatis* and *M. tuberculosis* are unusual in apparently being endowed with both MTAN and MTAP enzymes (20–21). Intriguingly, *Rv0535* (*pnp*) which was enzymatically established to encode an MTA phosphorylase in *M. tuberculosis* (21), lies in the genomes of the MTX-producing species *M. tuberculosis* and *M. avium* in close vicinity to ORFs potentially encoding an NAD-dependent nucleotide sugar epimerase (Rv0536), two glycosyltransferases (Rv0539 and Rv0541c) and a protein with structural similarity to a wide range of enzymes that transfer nucleotides onto phosphosugars (Rv0540) [Fig. 2]. Rv0539 (hereafter referred to as MtxS; 210 amino acid residues) is predicted to be an inverting GT-2 glycosyltransferase and therefore shares significant sequence similarities with polyprenyl-monophosphosugar synthases from *M. tuberculosis*, including the polyprenyl-monophosphomannose synthase Ppm1 (Rv2051c; 33% identity and 49% similarity on a 214 amino acid overlap) and the polyprenyl-monophospho-*N*-acetylgalactosaminyl synthase PpgS (Rv3631; 33% identity and 47% similarity on a 115 amino acid overlap). Rv0541c (hereafter referred to as MtxT) is predicted to be a GT-C superfamily glycosyltransferase dependent on decaprenyl-phosphate-linked sugar donors rather than nucleotide-sugar donors (22). *pnp* and *Rv0536* are likely to be co-transcribed as would be *mtxS* and *Rv0540*. This cluster of genes was not found in *M. leprae*, a species known to be devoid of the MTX motif on ManLAM (23). However, the five genes are conserved in the genomes of *M. kansasii, M. smegmatis*, many other slow- and fast-growing *Mycobacterium* species (*M. avium* complex species, *M. vanbaalenii, M. marinum, M. ulcerans*, etc.), as well as a number of other Actinomycetes, particularly *Rhodococcus* and *Streptomyces* [Fig. 2]. The conservation, syntenic arrangement and

sequence similarities of these ORFs to genes involved in the detoxification of MTA and the further processing of sugar residues was suggestive of their participation in the formation of the MTX capping motif of ManLAM. Based on what is known of the biogenesis of polysaccharides in mycobacteria in general (3), and that of the mannoside caps of ManLAM and galactosamine substituent of arabinogalactan in particular (24–26), it is indeed reasonable to assume that the formation of the MTX motif of ManLAM is topologically split across the plasma membrane and proceeds through a three-step mechanism as shown in the proposed biosynthetic model presented in Figure 3. The initial cytoplasmic enzymatic reactions would lead to the formation of a 5′-methylthioribose (MTR) nucleotide sugar followed by that of decaprenyl-phosphoryl-MTX (DP-MTX). DP-MTX would then be translocated from the cytosolic to the periplasmic face of the plasma membrane by a dedicated translocase, and the MTX motif finally transferred from DP-MTX to the *t*-Man*p* residue of the mannoside caps of ManLAM by a lipid-linked sugar-dependent glycosytransferase (3,22). Although the epimerization at C-3 of the ribose residue leading to the *xylo*-configured sugar donor may occur at different stages of the pathway, i.e., directly on MTA as has been reported in the nudibranch mollusk *Doris verrucosa* (27), at the level of 5′-methylthioribose-1-phosphate or at that of the nucleotide- or decaprenyl-phosphate-linked sugar donors, the sequence similarity that Rv0536 shares with nucleotide sugar epimerases suggests that the reactions leading to DP-MTX from MTA follow the sequential order presented in Fig. 3.

The genetic inactivation of mtxS and mtxT abolishes the synthesis of the MTX motif of ManLAM in M. tuberculosis

To investigate the putative involvement of the glycosyltransferases MtxS and MtxT in the formation of the MTX motif of ManLAM, the genes encoding these enzymes were disrupted by allelic replacement in *M. tuberculosis* H37Rv [Fig. 4]. The two mutants displayed wild-type (WT) morphotypes and grew similarly to their *M. tuberculosis* H37Rv parent strain on agar plates (data not shown). Genetic complementation was achieved by transforming the *mtxT* knock-out mutant with pMVGH1*mtxT*, and the *mtxS* mutant with both pMVGH1*mtxS* and pMVGH1[*mtxS-Rv0540*] since the operon-like structure of *mtxS-Rv0540* raised concerns of a polar effect of the inactivation of *mtxS* on the expression of *Rv0540*.

ManLAM was prepared from the WT, mutant and complemented mutant strains and analyzed for the presence of MTX motif by NMR spectroscopy (12–13). H-1 signals corresponding to 5′-methylthiopentose at δ 5.21 and corresponding oxidation products (5′-methylsulfoxypentose) at δ 5.25 and δ 5.27 were observed in the anomeric region of the 1-D ^{1}H NMR spectrum of the WT strain. The corresponding complete spin systems were further identified in the TOCSY spectrum [Fig. 5]. Indicative of the involvement of MtxS and MtxT in the synthesis of the MTX motif of ManLAM, these correlations were not observed in the *mtxS* and *mtxT* knock-out mutants [Fig. 5]. They were, however, restored in the complemented *mtxT* mutant [Fig. 5]. Perhaps due to the insufficient level of expression of *mtxS* and *mtxS-Rv0540* from the pMVGH1 plasmid in *M. tuberculosis*, attempts to complement H37RvΔ*mtxS* with either one of these plasmids have thus far failed to restore

the synthesis of the MTX motif of ManLAM to detectable levels in this mutant [Supplementary Figure 1].

Effect of inactivating mtxT on the DP-MTX content of M. tuberculosis cells

To further investigate the reason for the absence of MTX motif on the ManLAM of the *M. tuberculosis mtxS* and *mtxT* mutants, we next sought to determine whether these two genes were involved in the synthesis or utilization of DP-MTX, the likely sugar donor used in the periplasmic transfer of MTX onto the mannoside caps of ManLAM. To this end, an LC/MS method allowing for the detection of DP-MTX in intact mycobacterial cells was first developed and applied to the analysis of the *M. tuberculosis* H37Rv WT, mutant and complemented mutant strains. Figures 6a–i show the extracted ion chromatograms and mass spectra for the $[M\text{-}H]^-$ ion of various decaprenyl-phosphoryl-sugars. The analysis was complicated by the fact that DP-MTX and decaprenyl-phosphoryl-mannose (DPM) have almost the same molecular weight (*m/z* 939.6307 for DP-MTX and *m/z* 939.6484 for DPM). Thus, both species appear on the extracted ion chromatographs. DP-MTX and DPM, however, separate by HPLC [Fig. 6b] and their difference in mass can be seen on the mass spectra [Fig. 6g and 6h]. The presence of a deprotonated ion typifying DP-MTX could not be detected in the *M. tuberculosis* WT parent strain [Fig. 6a], the *mtxS* knock-out mutant or the *mtxS* knock-out complemented with *mtxS-Rv0540* [Supplementary Figure 2]. In sharp contrast, the *mtxT* knock-out mutant showed a clear accumulation of DP-MTX [Fig. 6b] and an oxidized form of DP-MTX, decaprenyl-phosphoryl-methylsulfoxyxylose (referred to as DP-MSX), with a deprotonated ion at *m/z* 955.6256 [Fig. 6e]. The build-up of DP-MTX and DP-MSX in H37RvΔ*mtxT* was partially reverted upon complementation with pMVGH1*mtxT* [Fig. 6c and 6f]. In line with the biosynthetic model proposed in Figure 3, the results of these analyses thus support the hypothesis that DP-MTX serves as a substrate for MtxT in the transfer of MTX to ManLAM.

To confirm the structures of DP-MTX and DP-MSX, their corresponding precursor ions at *m/z* 939.6307 and *m/z* 955.6256 were selected and analyzed by LC-MS/MS in the negative mode with a collision energy of 65 V. Figures 7a and 7b display the mass spectra of fragment ions obtained for DP-MTX and DP-MSX and, for comparative purposes, Fig. 7c and 7d display the fragmentation patterns of decaprenyl-phosphoryl-arabinose (DPA) and DPM, respectively. All decaprenyl-phosphoryl-sugar spectra present characteristic fragment ions at *m/z* 777.59 and 819.60 (28–29). The fragment ion at *m/z* 777.59 arises from the cleavage of the glycosidic bond as shown in Fig. 7a–d. Similarly, the fragment ion at *m/z* 819.60 corresponds to the cross-ring cleavage of their glycosyl residues between the ring oxygen and C-1 and between C-2 and C-3 as shown in Fig. 7a–d. The finding of these two ions in DP-MTX and DP-MSX [Fig. 7a–b] is thus consistent with these products being decaprenyl-phosphoryl-sugars. The resulting decaprenyl-phosphate ion at *m/z* 777.59 (DP-MTX) further fragments and yields a sequential loss of isoprene units with *m/z* 165.03, 233.10, 301.16. In a similar fashion, two fragment ions separated by 68 mass units containing isoprene phosphate at *m*/z 164.02 and 232.08 were present on the DP-MSX spectrum. Most importantly, the cleavage between the oxygen of the phosphate group and the polyisoprene unit (with a hydrogen transfer) shows the molecular weight of the glycosyl residue, as seen at *m/z* 258.99 for DP-MTX and at *m/z* 274.99 for DP-MSX. Fragments

containing the glycosyl residue for DP-MTX are further seen at *m/z* 325.05, 325.06, 394.12 and 461.18 [Fig. 7a], and at *m/z* 341.04 and 342.05 for DP-MSX [Fig. 7b]. Additionally, ions typifying the loss of the sulfur substituent are seen for both DP-MTX and DP-MSX (diagnostic ions at *m/z* 279.06) [Fig. 7a–b]. The MS/MS results are therefore consistent with the proposed structures.

In further support of the identity of DP-MTX and DP-MSX with formula $C_{56}H_{93}O_7PS$ and $C_{56}H_{93}O_8PS$, respectively, is the isotopic distribution of the $[M-H]^-$ ion observed in the ESI-TOF mass spectra. Compounds containing sulfur exhibit a characteristic isotopic distribution with a greater relative intensity at the M+2 ion than compounds without S, due to the relatively high natural abundance of ^{34}S (4.2 %) (30). The modeled isotopic distribution for $C_{56}H_{92}O_7PS$ ($[M-H]^-$) predicts the M+2 ion at *m/z* 941.6353 at a relative intensity of 25.2 %, whereas the modeled isotopic distribution of DPM, with formula $C_{56}H_{92}O_9P$ ($[M-H]^-$) predicts the relative intensity of the M+2 ion at 20.7 %. The difference of 4.5 % is explained by the combined number of molecules containing ^{34}S instead of ^{32}S, plus minor contributions from ^{18}O, ^{2}H and $^{13}C_2$. Similarly, the predicted relative intensity of the M+2 ion for DP-MSX ($[M-H]^-$) at *m/z* 957.6302 is 25.5 %. The good fit of the formula $C_{56}H_{92}O_7PS$ for DP-MTX ($[M-H]^-$) and $C_{56}H_{92}O_8PS$ for DP-MSX ($[M-H]^-$) with expected and observed isotopic distributions is illustrated with the overlaid modeled and observed data in the mass spectra [Supplementary Figure 3].

Effect of overexpressing mtxS on the DP-MTX content of M. smegmatis

The absence of detectable amounts of DP-MTX in *M. tuberculosis* H37Rv WT making a direct comparison of the DP-MTX content of the WT and *mtxS* knock-out uninformative [Supplementary Figure 2], we set out to overexpress *mtxS* to gain further insights into the function of this gene. *M. smegmatis* rather than *M. tuberculosis* was used as a model organism in these experiments because greater levels of expression of *mtxS* were achieved in this species [Fig. 8a] and the presence of DP-MTX in WT *M. smegmatis* cells [Fig. 8b] indicated that the four genes required for the synthesis of DP-MTX from MTA [Fig. 2 and Fig. 3] are functional in this species. Overexpression of the *M. tuberculosis mtxS* gene from pMVGH1*mtxS* in *M. smegmatis* consistently resulted in a 1.4-fold increase in the production of DP-MTX in the cells [Fig. 8b–c]. This effect was even more pronounced in an *M. smegmatis* recombinant strain co-expressing *mtxS* and the putative 5′-methylthioribose-1-phosphate nucleotidyl transferase gene (*Rv0540*) from pMVGH1[*mtxS-Rv0540*] indicating that the formation of NDP-MTR may be a rate-limiting step in the pathway. The amount of DP-MTX and DP-MSX detected in the membranes of this overexpressor was about 2.1-fold that measured in the membranes of the *M. smegmatis* control strain, *Msmg*/pMVGH1 [Fig. 8b–c]. Collectively, the build-up of DP-MTX in *M. smegmatis* strains overexpressing *mtxS*, the sequence resemblance that MtxS shares with other polyprenyl-monophosphosugar synthases from *M. tuberculosis*, and the fact that disrupting *mtxS* abolishes the formation of the MTX motif of ManLAM strongly support MtxS as the DP-MTX synthase of the pathway.

CONCLUSIONS

Altogether, our genetic and biochemical data validate the hypothesis that the MTX motif of *M. tuberculosis* ManLAM arises from a byproduct of spermidine biosynthesis and indicate that the formation and transfer of this motif proceeds through the overall biosynthetic scheme depicted in Fig. 3. The processes involved in the covalent modification of ManLAM with this unique thiosugar bear obvious resemblance to that responsible for the formation of the galactosaminyl substituent of arabinogalactan wherein a polyprenyl-phospho-*N*-acetyl galactosamine synthase encoded by PpgS (homologous to MtxS) generates the lipid-linked sugar donor used by Rv3779 (homologous to MtxT) for transfer onto arabinogalactan on the periplasmic side of the plasma membrane (26). Despite these significant advances in our understanding of the origin of the MTX motif, a number of outstanding questions about its synthesis and transfer to ManLAM remain. Among them is the identity of the translocase involved in the translocation of DP-MTX from the cytoplasmic to the periplasmic side of the inner membrane and the precise nature of the nucleotide-MTX donor used by MtxS in the formation of DP-MTX, whether UDP-MTX, GDP-MTX or otherwise.

The conservation of the core five genes of the pathway (*pnp, Rv0536, mtxS, Rv0540* and *mtxT*) in slow- and fast-growing *Mycobacterium* species, including *M. smegmatis* mc^2155 in which no MTX motif has yet been reported, as well as a number of other Actinomycetes suggests that the MTX motif, may be more widespread than previously appreciated. Whether the MTX motif may substitute other molecules than LM- and LAM-like polysaccharides, including glycoproteins and secondary metabolites, remains to be determined. This finding also brings into question the putative biological significance of this motif. The important impact that discrete glycosyl substituents have on the biological activities of bacterial lipopolysaccharides and teichoic acids, and the interactions of bacterial pathogens with their host is well documented (31–33). The restricted distribution of the MTX motif of ManLAM to pathogenic *Mycobacterium* species, its conservation in all *M. tuberculosis* isolates analyzed to date and exposure on the cell surface all point to an important role in immunopathogenesis. The MTX-deficient *M. tuberculosis* mutants generated in the course of this work open the way to host-pathogen interaction studies aimed at testing this hypothesis.

METHODS

Bacterial strains and growth conditions

M. tuberculosis H37Rv ATCC 25618 was grown at 37°C in Glycerol-Alanine-Salts (GAS) medium, Middlebrook 7H9 medium supplemented with 10% oleic acid-albumin-dextrose-catalase (OADC, BD Sciences) and 0.05% Tween 80, or Middlebrook 7H11 agar supplemented with 10% OADC. *M. smegmatis* mc^2155 was grown at 37°C in Luria Bertani (LB) medium (Difco). Kanamycin (Kan) and hygromycin (Hyg) were added to final concentrations of 25 μg mL^{-1} and 50 μg mL^{-1}, respectively.

Generation of M. tuberculosis knock-out and complemented knock-out mutants

The *mtxS* gene and flanking regions were PCR-amplified from *M. tuberculosis* H37Rv genomic DNA using primers Rv0539.1 (5'-gatacttctagatcgctcggcgccgttgagcc-3') and Rv0539.2 (5'-gatacttctagagatccggctgccatctgctgc-3') and a disrupted allele, *mtxS::kan*, was obtained by inserting the *Tn903* kanamycin resistance cassette at the NcoI restriction site of *mtxS*. *mtxS::kan* was then cloned in the XbaI-cut pPR27-*xylE*, yielding pPR27*mtxS*KX. The *mtxT* gene and flanking regions were PCR-amplified using primers Rv0541c.1 (5'-gatacttctagagcagctggctgttggctgtgc-3') and Rv0541c.2 (5'-gatacttctagagctggcgtgtcgtcgaactcg-3') and a disrupted allele, *mtxT::kan*, was obtained by replacing 924 bp of the *mtxT* ORF flanked between two BlpI restriction sites with the kanamycin resistance gene from *Tn903*. *mtxT::kan* was then cloned in the XbaI-cut pPR27-*xylE*, yielding pPR27*mtxT*KX. The Ts/*sacB* method was used to achieve allelic replacement at the *Rv0539* (herein renamed *mtxS*) and *Rv0541c* (herein renamed *mtxT*) loci of *M. tuberculosis* H37Rv (34). Allelic replacement at the *mtxS* and *mtxT* chromosomal loci was verified by PCR using upstream and downstream primers located outside the allelic exchange substrates.

For complementation studies and expression in *M. smegmatis*, the entire coding sequences of *mtxS* and *mtxT* were PCR-amplified from *M. tuberculosis* H37Rv genomic DNA and cloned into the replicative expression plasmid pMVGH1 (35), yielding pMVGH1*mtxS* and pMVGH1*mtxT*, respectively. pMVGH1[*mtxS-Rv0540*] was generated by amplifying the *mtxS* and *Rv0540* genes together and cloning the resulting PCR fragment in the same expression plasmid. These constructs allow for the constitutive expression of C-terminally hexahistidine-tagged MtxS, MtxT or Rv0540 proteins under control of the *hsp60* promoter. Primer sequences for these constructs are available upon request.

Lipid and lipoglycan extraction

Total lipid and lipoglycan extractions and LAM purification from mycobacterial cells followed earlier procedures (25).

Analytical procedures

LC-MS analyses were conducted on an Agilent 1200 binary pump liquid chromatograph (Agilent technologies/ Palo Alto, CA), using a 2.1 inner diameter × 150 mm, 3.5 μm XBridge reverse phase C18 column (Waters) heated to 45 °C as described (36). Decaprenyl phosphoryl-sugars were detected using an Agilent 6220A time-of-flight (TOF) mass spectrometer equipped with an electrospray ionization/atmospheric pressure chemical ionization (ESI/APCI), and a multimode source operated in the negative ion mode. Mass spectra were acquired at a rate of 1.02 spectra/second from *m/z* 250 to 3,200 Da and the data collected analyzed using the Mass Hunter software (Agilent).

Modeled isotopic distributions for DP-MTX and DP-MSX were calculated, overlaid with observed data, and visualized with the Isotope Distribution Calculator (Agilent MassHunter Workstation Data Analysis Core Version 4.0.479.0).

LC-MS/MS analyses were performed on an Agilent binary pump G4220A LC using a 2.1 × 100 mm, 2.6 μm Agilent Poroshell 120 EC-C18 column heated to 40 °C. Five μL of total lipid extracts were injected with an autosampler and separated at a flow rate of 0.3 mL min^{-1} as described (36). Decaprenyl phosphoryl-sugars were detected using an Agilent 6530 QTOF mass spectrometer equipped with electrospray ionization and a Jet Stream source operated in the negative ion mode. Precursor ions *m/z* 909.6379 (DPA), *m/z* 939.6307 (DP-MTX), *m*/z 939.6484 (DPM) and *m/z* 955.6256 (DP-MSX) were selected and fragmented using a collision energy setting of 65 V. Mass spectra were acquired at a rate of 1.0 spectrum/second from *m/z* 100 to 1,700 Da and the data collected analyzed using the Mass Hunter software (Agilent).

NMR spectra were recorded at 315 K on a Bruker Avance 600 MHz spectrometer equipped with a cryogenic probe TCi (Bruker Biospin, Germany). Purified ManLAM samples were exchanged in D_2O (D, 99.97 % from Euriso-top, Saint-Aubin, France), with intermediate lyophilization, and then dissolved in 0.5 mL DMSO (D, 99.96 % from Euriso-top, Saint-Aubin, France). Samples were analyzed in a 200 × 5 mm UL-5 NMR tube (Euriso-Top). Proton chemical shifts are expressed in part per million (ppm) and referenced relative to internal DMSO at 2.52 ppm. All 2D NMR data sets were recorded without sample spinning. $^{1}H–^{1}H$ correlation spectra were acquired in the echo/antiecho-TPPI gradient selection mode (512 data points) using the “mlevetgp” sequence from the Topspin v2.1 software (Bruker Biospin).

Supplementary Material

Refer to Web version on PubMed Central for supplementary material.

Acknowledgments

This work was supported by the National Institute of Allergy and Infectious Diseases/National Institutes of Health grant AI064798 (to M. Jackson), and the Alberta Glycomics Centre. The content is solely the responsibility of the authors and does not necessarily represent the official views of the NIH. The IPBS NMR equipment was financed by the French Research Ministry, CNRS, Université Paul Sabatier, the Région Midi- Pyrénées and the European structural funds. We thank D. Dick, T. Sours and B. Cranmer (Colorado State University) for their help with LC/MS and MS/MS analyses.

REFERENCES

1. Ortalo-Magné A, Lemassu A, Lanéelle MA, Bardou F, Silve G, Gounon P, Marchal G, Daffé M. Identification of the surface-exposed lipids on the cell envelopes of *Mycobacterium tuberculosis* and other mycobacterial species. J. Bacteriol. 1996; 178:456–461. [PubMed: 8550466]
2. Pitarque S, Larrouy-Maumus G, Payré B, Jackson M, Puzo G, Nigou J. The immunomodulatory lipoglycans, lipoarabinomannan and lipomannan, are exposed at the mycobacterial cell surface. Tuberculosis. 2008; 88:560–565. [PubMed: 18539533]
3. Angala SK, Belardinelli JM, Huc-Claustre E, Wheat WH, Jackson M. The cell envelope glycoconjugates of Mycobacterium tuberculosis. Crit. Rev. Biochem. Mol. Biol. 2014; 49:361–399. [PubMed: 24915502]
4. Kaur D, Angala SK, Wu SW, Khoo KH, Chatterjee D, Brennan PJ, Jackson M, McNeil MR. A single arabinan chain is attached to the phosphatidylinositol mannosyl core of the major immunomodulatory mycobacterial cell envelope glycoconjugate, lipoarabinomannan. J. Biol. Chem. 2014; 289:30249–30256. [PubMed: 25231986]

5. Shi L, Berg S, Lee A, Spencer JS, Zhang J, Vissa V, McNeil MR, Khoo K-H, Chatterjee C. The carboxy terminus of EmbC from *Mycobacterium smegmatis* mediates chain length extension of the arabinan in lipoarabinomannan. J. Biol. Chem. 2006; 281:19512–19526. [PubMed: 16687411]
6. Hunter SW, Gaylord H, Brennan PJ. Structure and antigenicity of the phosphorylated lipopolysaccharide antigens from the leprosy and tubercle bacilli. J. Biol. Chem. 1986; 261:12345–12351. [PubMed: 3091602]
7. Delmas C, Gilleron M, Brando T, Vercellone A, Gheorghiu M, Rivière M, Puzo G. Comparative structural study of the mannosylated-lipoarabinomannans from *Mycobacterium bovis* BCG vaccine strains: characterization and localization of succinates. Glycobiology. 1997; 7:811–817. [PubMed: 9376683]
8. Gilleron, M., Jackson, M., Nigou, J., Puzo, G. Structure, activities and biosynthesis of the Phosphatidyl-*myo*-Inositol-based lipoglycans. In: Daffé, M., Reyrat, J-M., editors. The Mycobacterial Cell Envelope. Washington, DC: ASM Press; 2008. p. 75-105.
9. Torrelles JB, Schlesinger LS. Diversity in Mycobacterium tuberculosis mannosylated cell wall determinants impacts adaptation to the host. Tuberculosis (Edinb). 2010; 90:84–93. [PubMed: 20199890]
10. Mishra AK, Driessen NN, Appelmelk BJ, Besra GS. Lipoarabinomannan and related glycoconjugates: structure, biogenesis and role in Mycobacterium tuberculosis physiology and host-pathogen interaction. FEMS Microbiol. Rev. 2011; 35:1126–1157. [PubMed: 21521247]
11. Neyrolles O, Guilhot C. Recent advances in deciphering the contribution of Mycobacterium tuberculosis lipids to pathogenesis. Tuberculosis (Edinb). 2011; 91:187–195. [PubMed: 21330212]
12. Treumann A, Xidong F, McDonnell L, Derrick PJ, Ashcroft AE, Chatterjee D, Homans SW. 5-methylthiopentose: a new substituent on liporabinomannan in *Mycobacterium tuberculosis*. J. Mol. Biol. 2002; 316:89–100. [PubMed: 11829505]
13. Ludwiczak P, Gilleron M, Bordat Y, Martin C, Gicquel B, Puzo G. *Mycobacterium tuberculosis phoP* mutant: lipoarabinomannan molecular structure. Microbiology. 2002; 148:3029–3037. [PubMed: 12368436]
14. Turnbull WB, Shimizu KH, Chatterjee D, Homans SW, Treumann A. Identification of the 5-methylthiopentose substituent in *Mycobacterium tuberculosis* lipoarabinomannan. Angew. Chem. Int. Ed. 2004; 43:3918–3922.
15. Joe M, Sun D, Taha H, Completo GC, Croudace JE, Lammas DA, Besra GS, Lowary TL. The 5-deoxy-5-methylthio-xylofuranose residue in mycobacterial lipoarabinomannan. Absolute stereochemistry, linkage position, conformation, and immunomodulatory activity. J. Am. Chem. Soc. 2006; 128:5059–5072. [PubMed: 16608340]
16. Turnbull WB, Stalford SA. Methylthioxylose--a jewel in the mycobacterial crown? Org. Biomol. Chem. 2012; 10:5698–5706. [PubMed: 22575989]
17. Guérardel Y, Maes E, Briken V, Chirat F, Leroy Y, Locht C, Strecker G, Kremer L. Lipomannan and lipoarabinomannan from a clinical isolate of *Mycobacterium kansasii:* Novel structural features and apoptosis-inducing properties. J. Biol. Chem. 2003; 278:36637–36651. [PubMed: 12829695]
18. Stalford SA, Fascione MA, Sasindran SJ, Chatterjee D, Dhandayuthapani S, Turnbull WB. A natural carbohydrate substrate for Mycobacterium tuberculosis methionine sulfoxide reductase A. Chem. Commun. (Camb). 2009:110–112. [PubMed: 19082015]
19. Chan J, Fan XD, Hunter SW, Brennan PJ, Bloom BR. Lipoarabinomannan, a possible virulence factor involved in persistence of *Mycobacterium tuberculosis* within macrophages. Infect. Immun. 1991; 59:1755–1761. [PubMed: 1850379]
20. Buckoreelall K, Wilson L, Parker WB. Identification and characterization of two adenosine phosphorylase activities in Mycobacterium smegmatis. J. Bacteriol. 2011; 193:5668–5674. [PubMed: 21821769]
21. Buckoreelall K, Sun Y, Hobrath JV, Wilson L, Parker WB. Identification of Rv0535 as methylthioadenosine phosphorylase from Mycobacterium tuberculosis. Tuberculosis (Edinb). 2012; 92:139–147. [PubMed: 22225784]

22. Berg S, Kaur D, Jackson M, Brennan PJ. The glycosyltransferases of *Mycobacterium tuberculosis*-roles in the synthesis of arabinogalactan, lipoarabinomannan, and other glycoconjugates. Glycobiology. 2007; 17:35R–56R. [PubMed: 17261566]
23. Torrelles JB, Khoo KH, Sieling PA, Modlin RL, Zhang N, Marques AM, Treumann A, Rithner CD, Brennan PJ, Chatterjee D. Truncated structural variants of lipoarabinomannan in Mycobacterium leprae and an ethambutol-resistant strain of Mycobacterium tuberculosis. J. Biol. Chem. 2004; 279:41227–41239. [PubMed: 15263002]
24. Dinadayala P, Kaur D, Berg S, Amin AG, Vissa VD, Chatterjee D, Brennan PJ, Crick DC. Genetic basis for the synthesis of the immunomodulatory mannose caps of lipoarabinomannan in *Mycobacterium tuberculosis*. J. Biol. Chem. 2006; 281:20027–20035. [PubMed: 16704981]
25. Kaur D, Obregón-Henao A, Pham H, Chatterjee D, Brennan PJ, Jackson M. Lipoarabinomannan of *Mycobacterium*; mannose capping by a multifunctional terminal mannosyltransferase. Proc. Natl. Acad. Sci. USA. 2008; 105:17973–17977. [PubMed: 19004785]
26. Škovierová H, Larrouy-Maumus G, Pham H, Belanova M, Barilone N, Dasgupta A, Mikušová K, Gicquel B, Gilleron M, Brennan PJ, Puzo G, Nigou J, Jackson M. Biosynthetic origin of the galactosamine substituent of Arabinogalactan in *Mycobacterium tuberculosis*. J. Biol. Chem. 2010; 285:41348–41355. [PubMed: 21030587]
27. Porcelli M, Cacciapuoti G, Cimino G, Gavagnin M, Sodano G, Zappia V. Biosynthesis and metabolism of 9-[5'-deoxy-5'-(methylthio)-beta-D-xylofuranosyl]adenine, a novel natural analogue of methylthioadenosine. Biochem. J. 1989; 263:635–640. [PubMed: 2512910]
28. Wolucka BA, McNeil MR, de Hoffmann E, Chojnacki T, Brennan PJ. Recognition of the lipid intermediate for arbinogalactan/arabinomannan biosynthesis and its relation to the mode of action of ethambutol on mycobacteria. J. Biol. Chem. 1994; 269:23328–23335. [PubMed: 8083238]
29. Wolucka BA, de Hoffmann E. Isolation and characterization of the major form of polyprenyl-phospho-mannose from *Mycobacterium smegmatis*. Glycobiology. 1998; 8:955–962. [PubMed: 9719676]
30. Budzikiewicz H, Grigsby RD. Mass spectrometry and isotopes: a century of research and discussion. Mass Spectrom. Rev. 2006; 25:146–157. [PubMed: 16134128]
31. Swoboda JG, Campbell J, Meredith TC, Walker S. Wall teichoic acid function, biosynthesis, and inhibition. ChemBioChem. 2010; 11:35–45. [PubMed: 19899094]
32. Needham BD, Trent MS. Fortifying the barrier: the impact of lipid A remodelling on bacterial pathogenesis. Nat. Rev. Microbiol. 2013; 11:467–481. [PubMed: 23748343]
33. Wheat WH, Dhouib R, Angala SK, Larrouy-Maumus G, Dobos K, Nigou J, Spencer JS, Jackson M. The presence of a galactosamine substituent on the arabinogalactan of Mycobacterium tuberculosis abrogates full maturation of human peripheral blood monocyte-derived dendritic cells and increases secretion of IL-10. Tuberculosis (Edinb). 2015; 95:476–489. [PubMed: 26048627]
34. Jackson, M., Camacho, LR., Gicquel, B., Guilhot, C. Gene replacement and transposon delivery using the negative selection marker *sacB*. In: Parish, T., Stocker, NG., editors. Mycobacterium tuberculosis protocols. Totowa N J: Humana Press; 2001. p. 59-75.
35. Grzegorzewicz AE, Pham H, Gundi VAKB, Scherman MS, North EJ, Hess T, Jones V, Gruppo V, Born SEM, Korduláková J, Chavadi SS, Morisseau C, Lenaerts AJ, Lee RE, McNeil MR, Jackson M. Inhibition of mycolic acid transport across the *Mycobacterium tuberculosis* plasma membrane. Nat. Chem. Biol. 2012; 8:334–341. [PubMed: 22344175]
36. Sartain MJ, Dick DL, Rithner CD, Crick DC, Belisle JT. Lipidomic analyses of *Mycobacterium tuberculosis* based on accurate mass measurements and the novel Mtb LipidDB. J. Lipid Res. 2011; 52:861–872. [PubMed: 21285232]

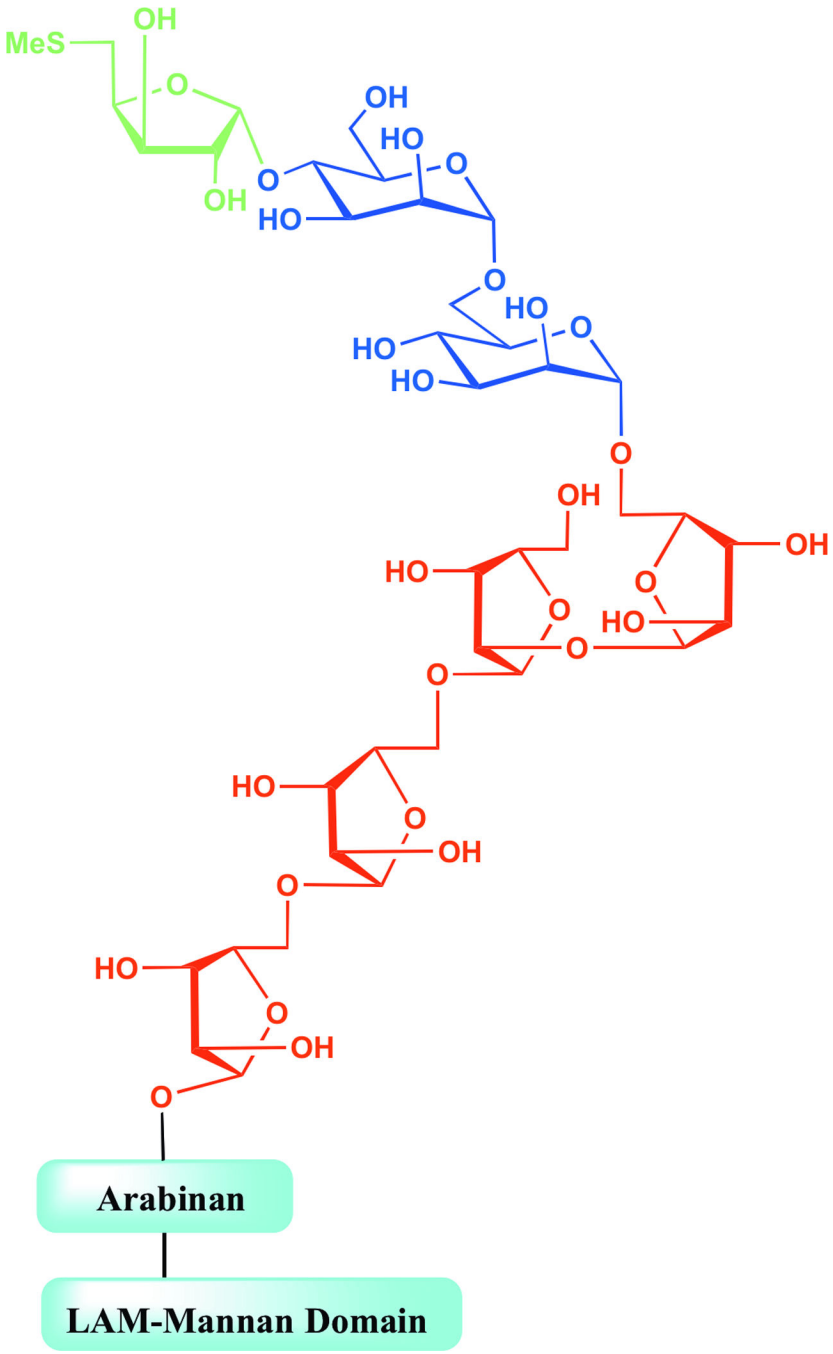

Figure 1. Representation of the non-reducing arabinan termini of *M. tuberculosis* ManLAM

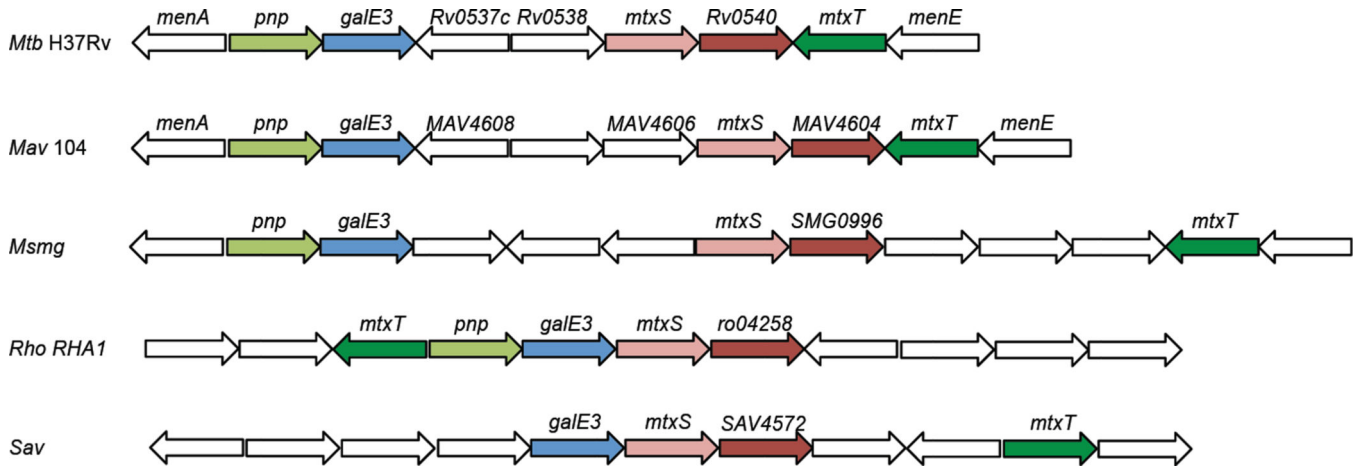

Figure 2. Representation of the MTX gene cluster in *M. tuberculosis* and other Actinomycetes

Mtb H37Rv, *Mycobacterium tuberculosis* strain H37Rv; *Mav* 104, *Mycobacterium avium* strain 104; *Msmg, Mycobacterium smegmatis* mc^2155; Rho RHA1, *Rhodococcus* sp. RHA1; Sav, *Streptomyces avermitilis* MA-4680. Similarly colored genes are orthologs. White genes are thought to be unrelated to the MTX biosynthetic pathway. Genes are not drawn to scale. Pnp, MTA phosphorylase; GalE3, putative NAD-dependent 5´-methylthioribose-nucleotide-3-epimerase; MtxS, decaprenyl-phosphoryl-MTX synthase; Rv0540 (and orthologs, MAV4604, SMG0996, ro04258, SAV4572), nucleotide-5´-methylthioribose synthase; MtxT, MTX-transferase. The *pnp* gene of *S. avermitilis* (SAV3679) is found in a different region of the genome. Rv0537c and MAV4608 display sequence similarities with the 5´-methylthioribose-1-phosphate isomerase from *Bacillus licheniformis* and are likely to be involved in the methionine salvage pathway. *Rv0538* encodes a conserved membrane protein; orthologs of this gene are lacking in the MTX clusters of *M. avium, M. smegmatis, S. avermitilis* and *Rhodococcus* RHA1.

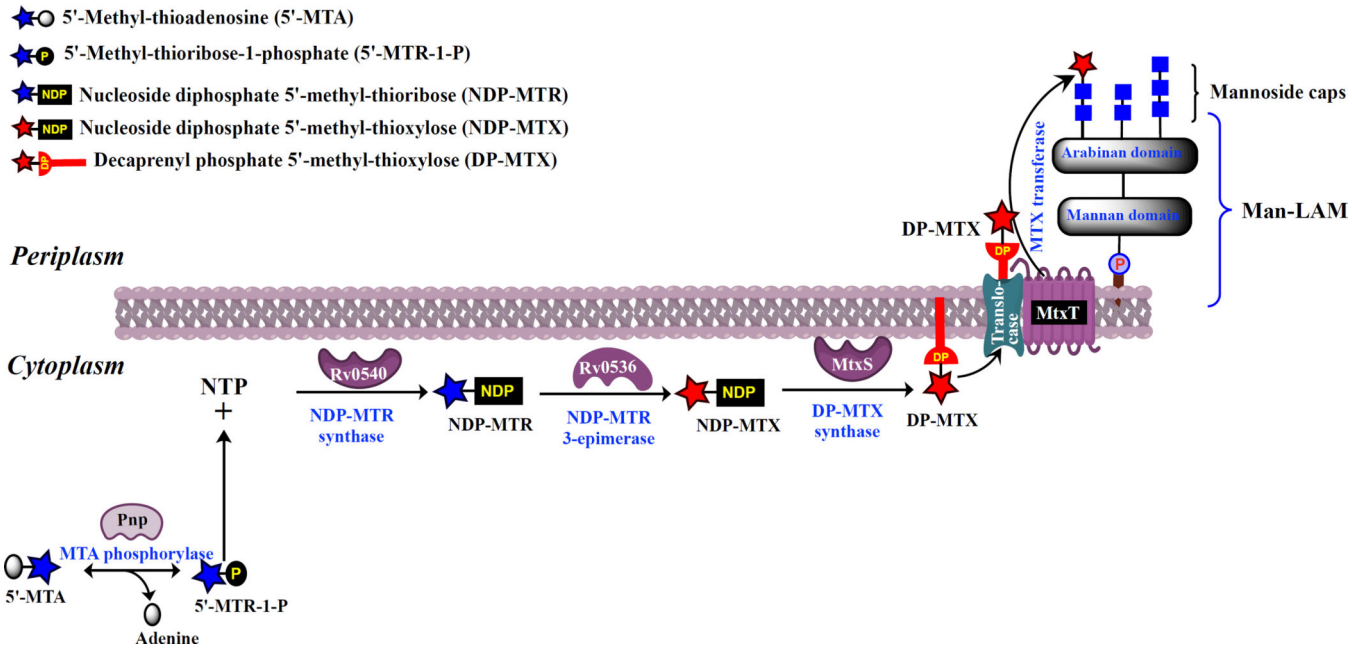

Figure 3. Proposed biosynthetic pathway for the formation of the MTX motif of ManLAM in *M. tuberculosis*

The proposed catalytic steps leading to the synthesis of the MTX motif and its transfer onto the mannoside caps of *M. tuberculosis* ManLAM are represented. The identity of the translocase involved in the translocation of DP-MTX from the cytoplasmic to the periplasmic side of the inner membrane and the precise nature of the nucleotide-MTX donor used by MtxS in the formation of DP-MTX are not known.

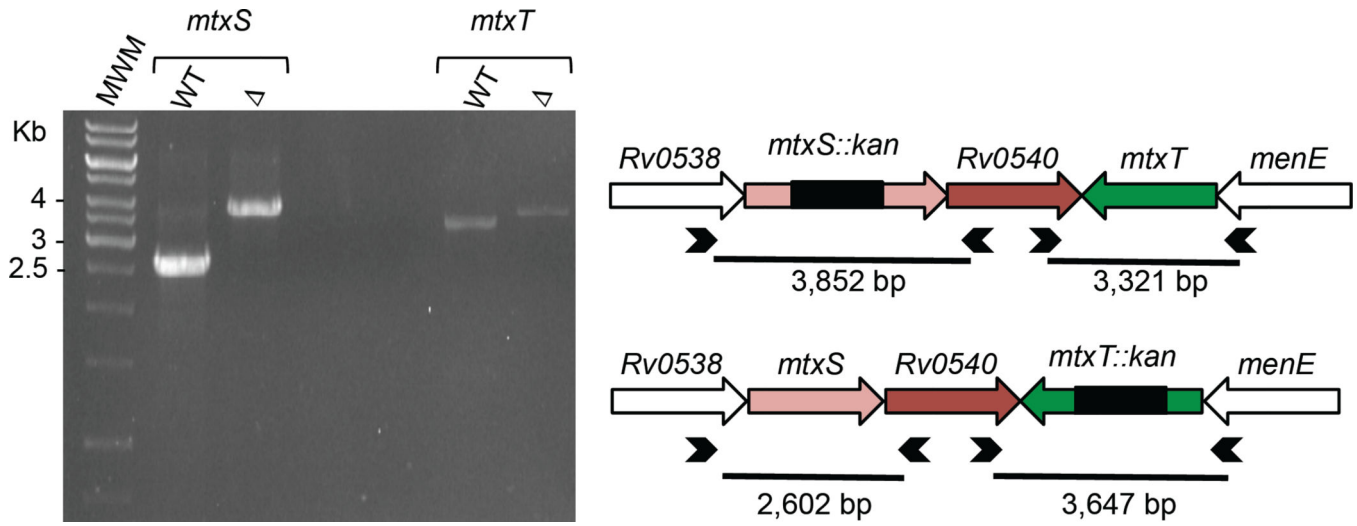

Figure 4. Allelic replacement at the *mtxS* and *mtxT* glycosyltransferase loci of *M. tuberculosis* H37Rv

Allelic replacement at the *mtxS* and *mtxT* loci of *M. tuberculosis* H37Rv was confirmed by PCR using sets of primers (represented as arrowheads) located outside the allelic exchange substrates. The WT 2,602 bp *mtxS* fragment is replaced by a 3,852-bp fragment in the *mtxS* knock-out mutant due to the insertion of a 1.2 kb-kanamycin resistance cassette at the unique NcoI restriction site of *mtxS*. The WT 3,321 bp *mtxT* fragment is replaced by a 3,647-bp fragment in the *mtxT* knock-out mutant due to a 1.2 kb-kanamycin resistance cassette replacing 924-bp of the *mtxT* gene flanked between two BlpI restriction sites in *mtxT*.

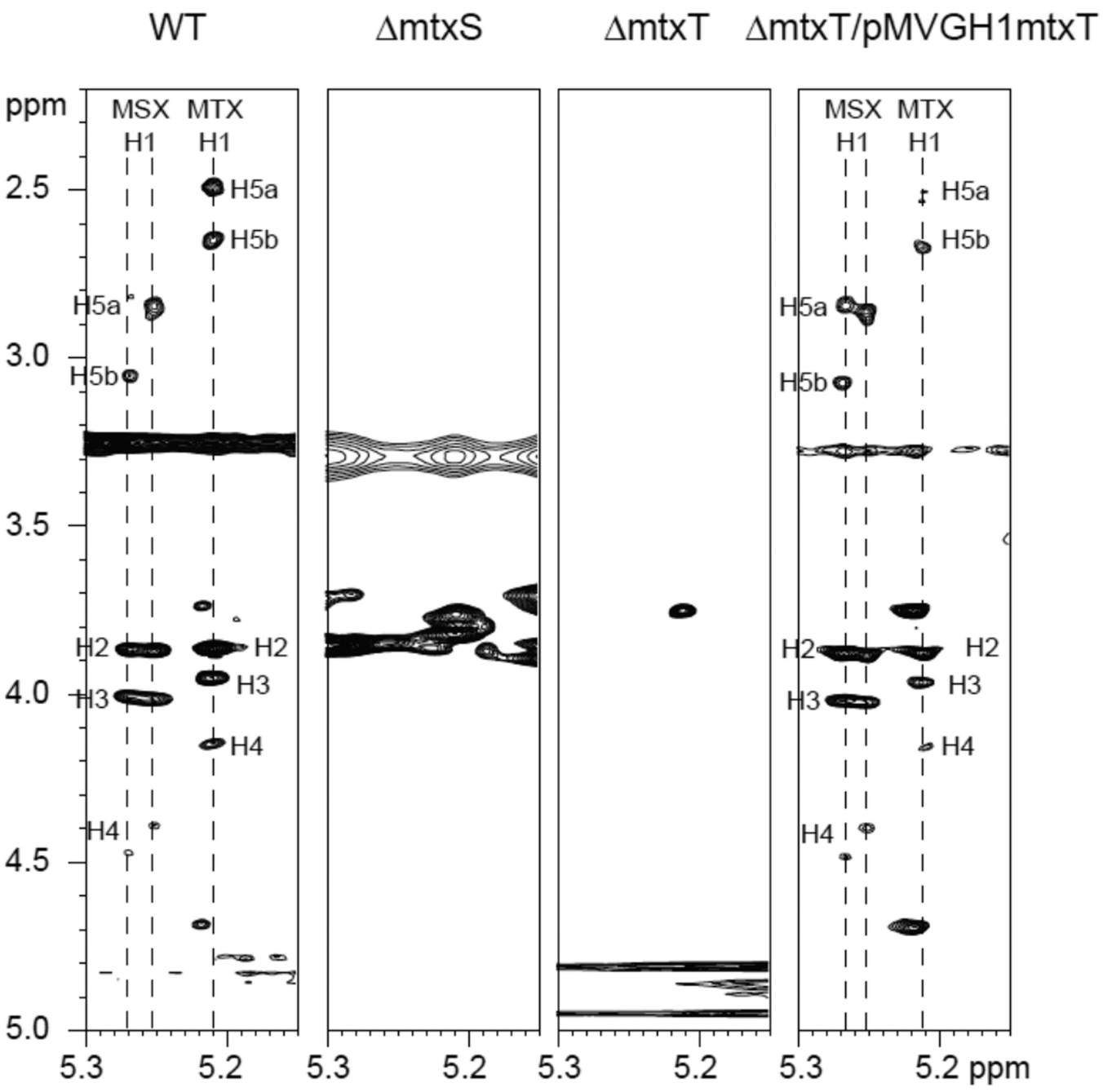

Figure 5. Expanded region of the 2D ^{1}H-^{1}H TOCSY spectrum in DMSO-d6 at 315 K of ManLAM purified from *M. tuberculosis* H37Rv WT, the *mtxS* and *mtxT* knock-out mutants and the complemented *mtxT* mutant strain

Coupling systems corresponding to 5′-methylsulfoxypentose and 5′-methylthiopentose (labeled as MSX and MTX, respectively) are presented. Numerals correspond to the proton number of the 5′-methylthiopentose and the 5′-methylsulfoxypentose units.

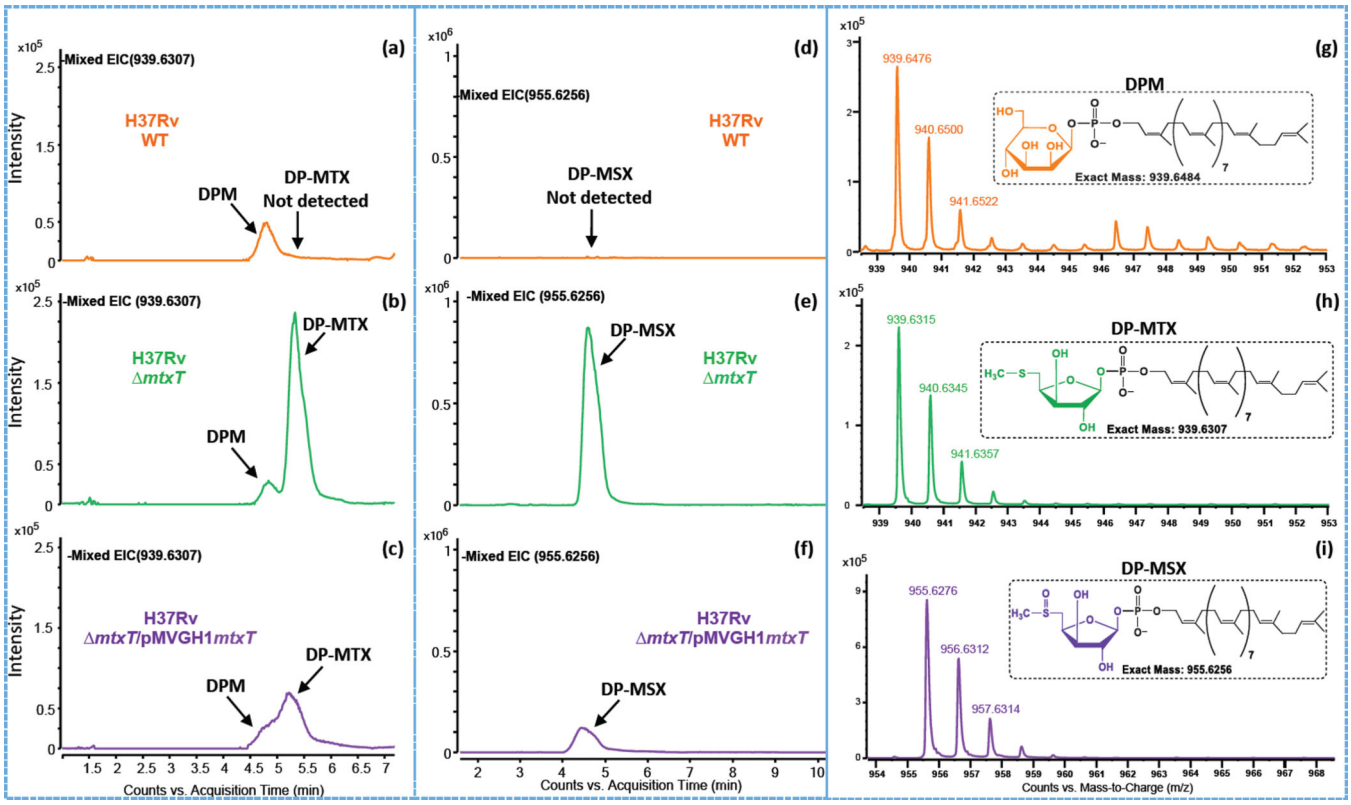

Figure 6. Negative ion LC/MS of decaprenyl-phosphoryl-sugars from total lipids extracts of *M. tuberculosis* H37Rv WT, the *mtxT* knock-out mutant and the complemented *mtxT* mutant strain

Panels (**a–c**) are the extracted ion chromatograms (EICs) of *m/z* 939.6307 showing the presence of DPM (actual $[M\text{-}H]^-$ at mass *m/z* 939.6484; see text for details) and the presence or absence of DP-MTX in the different *M. tuberculosis* strains. The detection of DP-MSX at *m/z* 955.6256 as $[M\text{-}H]^-$ ions are shown in the EICs presented in panels **d–f**. The insets in the mass spectra shown in panels (**g–i**) show the possible structures and the exact mass of the $[M\text{-}H]^-$ ions of the decaprenyl-phosphoryl sugars detected.

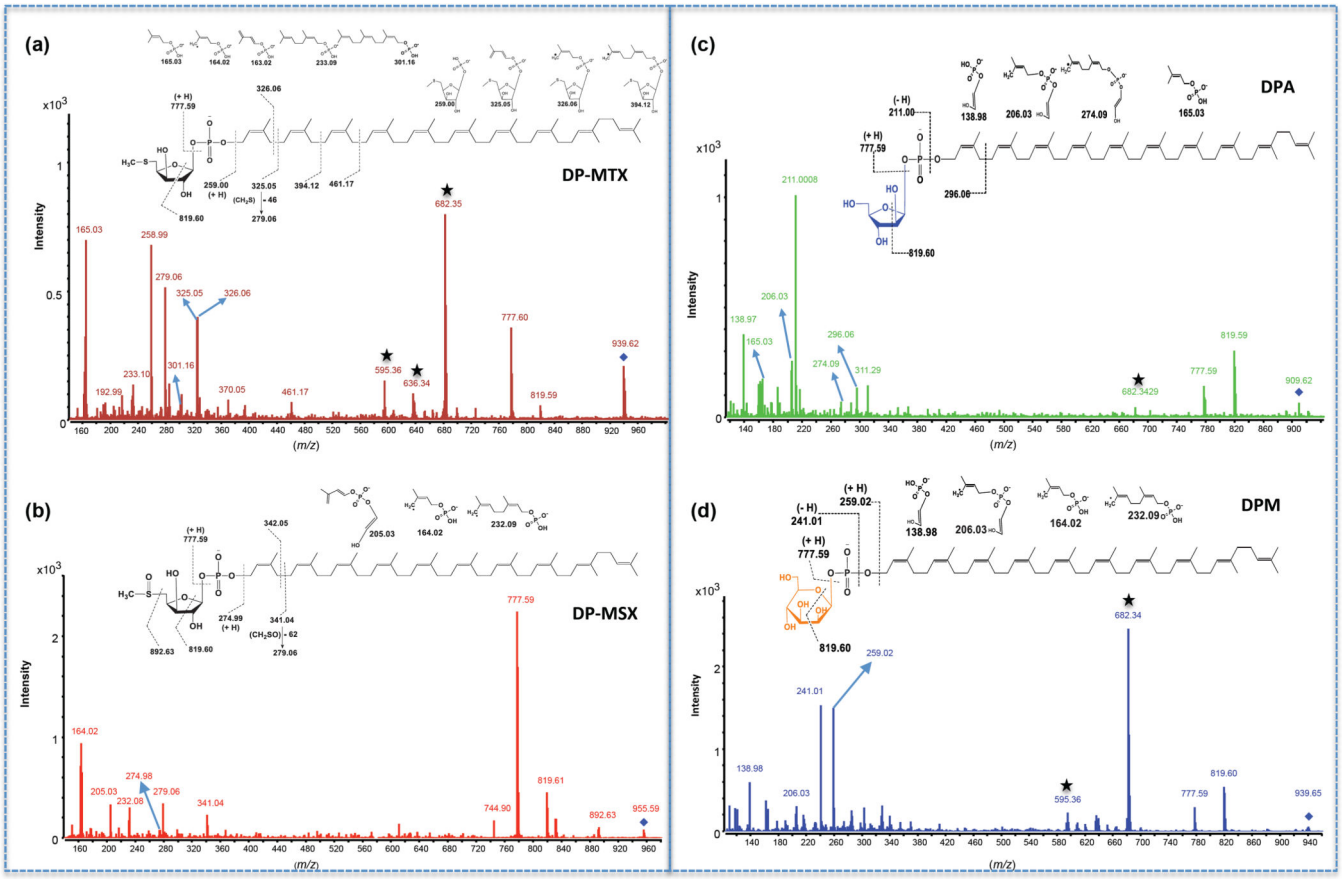

Figure 7. LC-MS/MS analysis of decaprenyl-phosphoryl sugars from total lipids extracts of the *M. tuberculosis* H37Rv *mtxT* knock-out mutant

MS/MS spectra and proposed fragmentation patterns of DP-MTX (**a**), DP-MSX (**b**), DPA (**c**) and DPM (**d**). The fragmented precursor $[M-H]^-$ ions are identified with a diamond. The details of the cleavages are discussed in the text. Ions labeled with stars come from the fragmentation of a contaminant ion with a mass close to the *m/z* value of 939.6307. For DP-MTX and DPM, this ion is at *m/z* 939.4671.

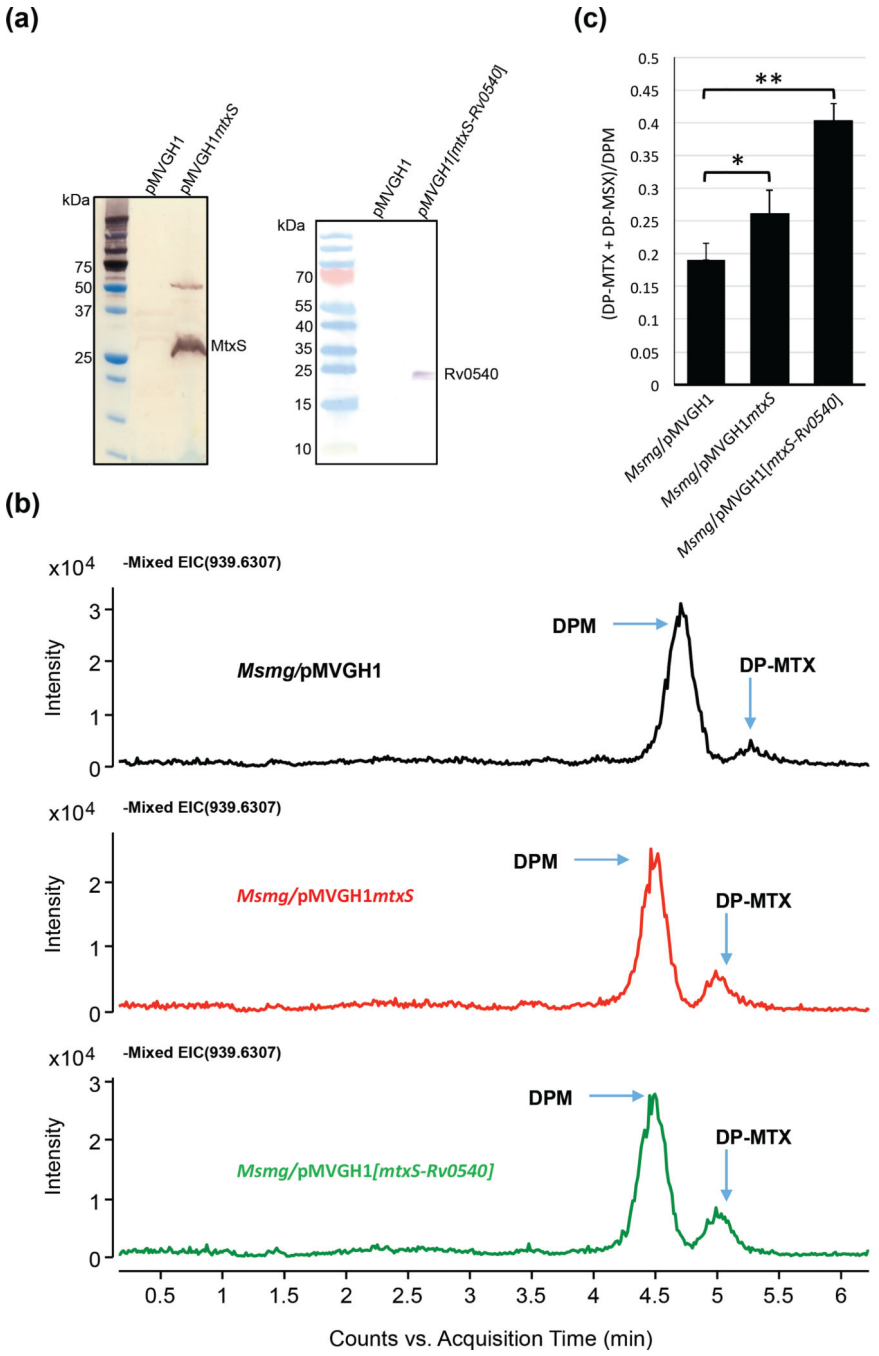

Figure 8. Effect of overexpressing *mtxS* and *mtxS-Rv0540* on DP-MTX synthesis in *M. smegmatis*

(**a**) Immunoblot analysis of MtxS and Rv0540 produced in *M. smegmatis*. *M. smegmatis* protein extracts prepared from *mtxS* and *mtxS-Rv0540* overexpressing strains and a control strain carrying an empty pMVGH1 plasmid were separated by SDS-PAGE, blotted onto a nitrocellulose membrane, and the recombinant proteins (harboring an C-terminal His-tag) were detected using a monoclonal anti-polyhistidine monoclonal antibody (mouse Ig2a isotype; Sigma) as the first antibody and an anti-mouse IgG-alkaline phosphatase-conjugated antibody as the secondary antibody. Immune complexes were detected by monitoring

alkaline phosphatase activity using NBT/BCIP (Thermo Scientific). The expected size of the recombinant Rv0540 protein is about 22.9 kDa; that of the recombinant MtxS protein is about 22.4 kDa; this protein consistently migrates with an apparent higher molecular weight, possibly due to its association with the membrane. A possible dimer of MtxS is also seen around 50 kDa.

(**b**) Negative ion LC/MS of DPM and DP-MTX from total lipids extracts of the *M. smegmatis* control strain (*Msmg*/pMVGH1) and the *mtxS* and *mtxS-Rv0540* overexpressors. Decaprenyl-phosphoryl sugars were analyzed as described in Fig. 6.

(**c**) Relative amounts of DP-MTX and its sulfoxide form, DP-MSX, in the membranes of the *M. smegmatis* control strain, *Msmg*/pMVGH1, the *mtxS* overexpressor and the *mtxS-Rv0540* overexpressor. The amounts of DP-MTX and DP-MSX relative to DPM were determined and the averages and standard deviations of two independent membrane preparations for each strain are shown. Statistical comparison (Student's *t*-test) between control and overexpressing strains: ** $p < 0.010$; * $p < 0.05$.